

Conformational Stabilities of 1,1-Dicyclopropylethene Determined from Variable-Temperature Infrared Spectra of Xenon Solutions and *ab Initio* Calculations

James R. Durig,^{*,‡} Chao Zheng,^{‡,†} Gamil A. Guirgis,[§] and Charles J. Wurrey[‡]

Department of Chemistry, University of Missouri–Kansas City, 5100 Rockhill Road, Kansas City, Missouri 64110, and Department of Chemistry & Biochemistry, College of Charleston, Charleston, South Carolina 29424

Received: September 13, 2004; In Final Form: December 8, 2004

The infrared (3200–40 cm^{-1}) spectra of gaseous and solid 1,1-dicyclopropylethene, $(c\text{-C}_3\text{H}_5)_2\text{C}=\text{CH}_2$, along with the Raman (3200–40 cm^{-1}) spectra of liquid and solid phases, have been recorded. The major *trans-gauche* (C=C bond *trans* to one ring with the other ring rotated about 60° from the C=C bond, trivial C_1 symmetry) and *gauche-gauche* (the two three-membered rings rotated oppositely about 60° from the C=C bond, C_2 symmetry) rotamers have been confidently identified in the fluid phases, but no definitive spectroscopic evidence was found for the *gauche-gauche'* form (the two three-membered rings rotated to the same side about 60° from the C=C bond, C_s symmetry), which is calculated to be present in no more than 6% at ambient temperature. Variable-temperature (-55 to -100°C) studies of the infrared spectra of the sample dissolved in liquid xenon have been carried out. Utilizing six different combinations of pairs of bands from the C_1 and C_2 conformers, the average enthalpy difference between these two has been determined to be $146 \pm 30 \text{ cm}^{-1}$ ($1.75 \pm 0.36 \text{ kJ}\cdot\text{mol}^{-1}$), with the C_1 form more stable. Given statistical weights of 2:1:1 respectively for the C_1 , C_2 , and C_s forms, it is estimated that there are $75 \pm 2\%$ C_1 and $19 \pm 1\%$ C_2 conformers present at ambient temperature. By utilizing predicted frequencies, infrared intensities, Raman activities, and band envelopes from scaled MP2(full)/6-31G(d) *ab initio* calculations, a complete vibrational assignment is made for the C_1 form and a number of fundamentals of the C_2 conformer have been identified. The structural parameters, dipole moments, and conformational stabilities have been obtained from *ab initio* calculations at the level of Hartree–Fock (RHF), the perturbation method to second order with full electron correlation (MP2(full)), and hybrid density functional theory (DFT) by the B3LYP method with a variety of basis sets. The predicted conformational stabilities from the MP2 calculations with relatively large basis sets are consistent with the experimental results. Structural parameters are estimated from the MP2(full)/6-311+G(d,p) predictions which are compared to the previously reported electron diffraction parameters. These experimental and theoretical results are compared to the corresponding quantities of some similar molecules.

Introduction

The monosubstituted methylcyclopropane molecules have been of interest to structural chemists and physicists for many years since there is the possibility of three different conformers, i.e., *cis* (*syn*), *trans* (*anti*), and *gauche*, being the most stable form. For example, cyclopropyl carboxaldehyde ($c\text{-C}_3\text{H}_5\text{CHO}$) has the *cis* and *trans* conformers^{1–5} as the two stable forms, while for the isoelectronic vinylcyclopropane ($c\text{-C}_3\text{H}_5\text{CH}=\text{CH}_2$) molecule the two stable conformers^{6–14} are the *trans* and the two equivalent *gauche* forms with the *trans* form reported¹³ to be more stable with an enthalpy difference of $500 \pm 50 \text{ cm}^{-1}$ ($5.98 \pm 0.60 \text{ kJ}\cdot\text{mol}^{-1}$). Whether vinylcyclopropane has a stable *cis* form has not been thoroughly investigated, although if this conformer does exist it must be in very small abundance at ambient temperature. Nevertheless, it is clear that there are significant differences in the conformational stabilities of monosubstituted vinyl and carbonyl cyclopropanes.

As a continuation of our studies of the conformational stabilities of substituted cyclopropanes, we initiated a vibrational and theoretical investigation of 1,1-dicyclopropylethene ($c\text{-C}_3\text{H}_5)_2\text{C}=\text{CH}_2$) with particular interest for comparison with the corresponding ketone, dicyclopropyl ketone ($c\text{-C}_3\text{H}_5)_2\text{C}=\text{O}$).¹⁵ In an earlier rather complete vibrational study¹⁶ of 1,1-dicyclopropylethene, the authors concluded that there was only one conformer present in both fluid phases at ambient temperature, which was the *cis-cis* (C_{2v}) conformer. This conclusion was consistent with two earlier studies^{17,18} in which only one conformer was observed. In one of these studies¹⁸ it was concluded that the *cis-cis* (C_{2v}) form was present from the solution dipole moment and molar Kerr constant measurements. The conclusions from the vibrational study¹⁶ were based on Raman depolarization data as well as the comparison between the Raman spectrum of the liquid phase with that of the crystalline solid. For the *cis-cis* C_{2v} form there should be 14 A_1 modes to give rise to polarized Raman lines whereas the *gauche-gauche* rotamer with C_2 symmetry (Figure 1) has 24 A modes and the *gauche-gauche'* form with C_s symmetry has 25 A' modes, so 24 or 25 polarized Raman lines are expected for the *gauche-gauche*(\pm) rotamers. The authors¹⁶ dismissed the possibility of the *cis-gauche* form on the basis that they expected

* Corresponding author. Phone: 01 (816)235-6038. Fax: 01 (816)235-2290. E-mail: durigj@umkc.edu.

[‡] University of Missouri–Kansas City.

[†] Taken in part from the thesis of C. Zheng, which will be submitted to the Department of Chemistry, University of Missouri–Kansas City, Kansas City, MO, in partial fulfillment of the Ph.D. degree.

[§] College of Charleston.

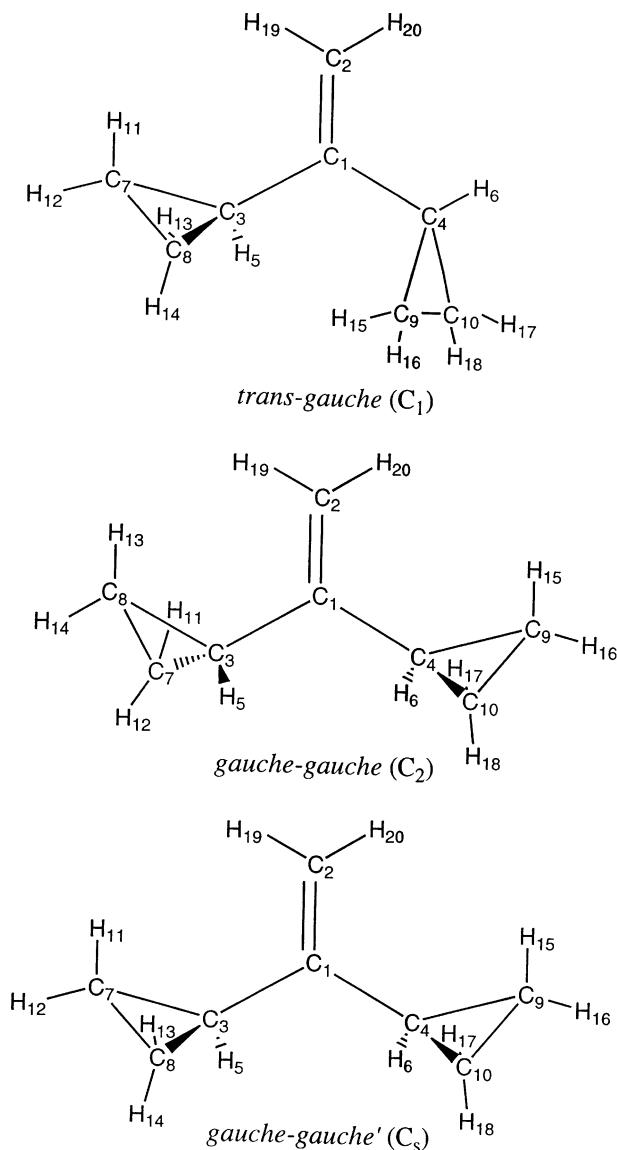


Figure 1. Geometric model with atom numbering for the three conformers of 1,1-dicyclopropylethene.

both rings to behave identically, and the trans-trans rotamer was concluded to be sterically impossible based on Dreiding stereomodels. Since 14 of the 25 observed Raman lines were found to be polarized and since little or no coupling was found between the two cyclopropyl rings so that in-phase and out-of-phase motions appeared as single lines, they¹⁶ stated that the 14 polarized Raman lines strongly supported the C_{2v} cis-cis structure. They¹⁶ also concluded that the broad bands in the spectra could be accounted for by the presence of two or more overlapping fundamental vibrations and that no band disappeared upon crystallization of the sample. However, a review of their reported Raman data does not appear to be consistent with this latter observation. For example, there is a very weak, broad Raman line at 1348 cm^{-1} in the spectrum of the liquid that disappears in the spectrum of the solid. Similarly the 800 cm^{-1} shoulder band present in the spectrum of the liquid is not present in the spectrum of the solid. Likewise three additional low-frequency bands at 700 (weak, shoulder), 411 (polarized, shoulder), and 290 (polarized, medium intensity) cm^{-1} in the spectrum of the liquid are not observed in the solid. The last one is of particular interest since it is of medium intensity and it is a low-frequency skeletal bending mode that should be most sensitive to the presence of more than one conformer in the

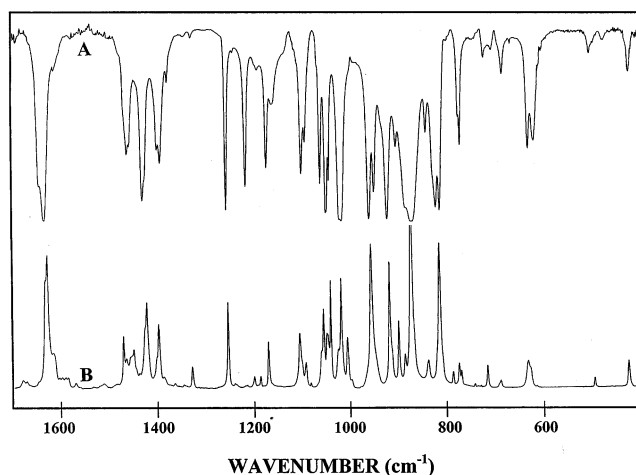


Figure 2. Infrared spectra of 1,1-dicyclopropylethene: (A) gas and (B) annealed solid.

fluid phases. Therefore we believed that the Raman lines which disappeared from the spectrum of the liquid with crystallization were in fact due to a second conformer and we, thus, have launched this investigation on the vibrational spectrum of 1,1-dicyclopropylethene with the expectation of finding more than one conformer in the fluid phases and furthermore to obtain conformational enthalpy difference by studying the temperature dependence of the intensity of fundamentals in xenon solutions.

To support the vibrational study we have carried out ab initio calculations with much larger basis sets than the 6-31G(d) used in a rather recent electron diffraction and theoretical investigation¹⁹ of 1,1-dicyclopropylethene. We have carried out calculations with basis sets up to 6-311G(2df,2pd) as well as those with diffuse functions, i.e. 6-311+G(2df,2pd). We found that there can be significant differences in the predicted stabilities of the $c\text{-C}_3\text{H}_5\text{CXO}$ molecules^{20–24} with the size of the basis set, particularly with the inclusion of diffuse functions at the MP2 level. We have also carried out density functional theory (DFT) calculations by the B3LYP method with the same basis sets. We have calculated optimized geometries, conformational stabilities, harmonic force fields, infrared intensities, Raman activities, and depolarization ratios. The results of these spectroscopic and theoretical studies are reported herein.

Experimental Section

The 1,1-dicyclopropylethene sample was purchased from Aldrich Chemical Co. with a stated purity of 95%. After several vacuum transfers the sample was found to be 99% pure by NMR. The sample was further purified with a low-pressure, low-temperature fractionation column and the purity of the sample was checked by a comparison of the infrared spectrum to the previously reported one.¹⁶ The purified sample was kept in the dark at low temperature until it was used.

The mid-infrared spectra of the gas (Figure 2A) and solid (Figure 2B) were obtained from 3200 to 220 cm^{-1} on a Perkin-Elmer model 2000 Fourier transform spectrometer equipped with a Ge/CsI beam splitter and a DTGS detector. Atmospheric water vapor was removed from the spectrometer housing by purging with dry nitrogen. The spectrum of the gas was obtained with the sample contained in a 12-cm cell fitted with CsI windows. The spectra of amorphous and crystalline solids were obtained by condensing the sample on a CsI substrate held at the temperature of boiling liquid nitrogen housed in a vacuum cell fitted with CsI windows. The sample was condensed as an

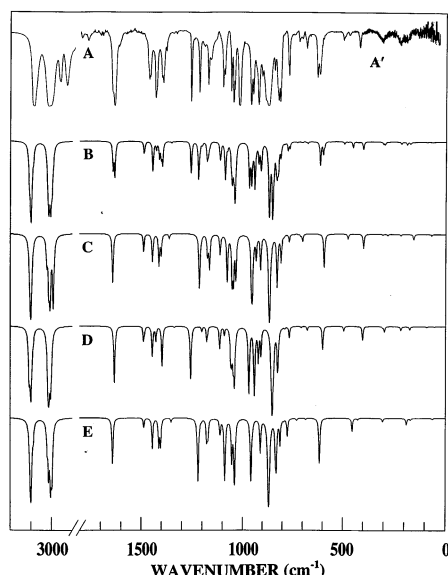


Figure 3. Infrared spectra of 1,1-dicyclopropylethene: (A) xenon solution at $-70\text{ }^{\circ}\text{C}$ (A', gas); (B) calculated spectrum of the mixture of the three conformers at $-70\text{ }^{\circ}\text{C}$ with ΔH of 146 and 350 cm^{-1} ; (C) calculated spectrum of the gauche-gauche', C_s conformer; (D) calculated spectrum of the gauche-gauche, C_2 conformer; and (E) calculated spectrum of the trans-gauche conformer.

amorphous solid and repeatedly annealed until no further changes were observed in the spectra. The theoretical resolution used to obtain the spectra of the gas and the solid was 0.5 and 2.0 cm^{-1} , respectively, and usually 128 interferograms were collected and averaged, and the data were transformed using a boxcar truncation function.

The mid-infrared spectra of the sample dissolved in liquefied xenon (Figure 3A) as a function of temperature were recorded on a Bruker model IFS 66 Fourier transform spectrometer equipped with a Globar source, a Ge/KBr beam splitter, and a DTGS detector. In all cases, 100 interferograms were collected at 1.0 cm^{-1} resolution, averaged, and transformed with a boxcar truncation function. For these studies, a specially designed cryostat cell was used. It consists of a copper cell with a path length of 4 cm with wedged silicon windows sealed to the cell with indium gaskets. The copper cell was enclosed in an evacuated chamber fitted with KBr windows. The temperature was maintained with boiling liquid nitrogen and monitored with two Pt thermoresistors. The complete cell was connected to a pressure manifold, which allowed the filling and evacuation of the system. After cooling to the desired temperature, a small amount of the compound was condensed into the cell. Next, the system was pressurized with xenon, which immediately started to condense in the cell, allowing the compound to dissolve.

The far-infrared spectrum (400 to 40 cm^{-1}) of the gas was recorded on the previously described Perkin-Elmer model 2000 spectrometer equipped with a metal grid beam splitter and a DTGS detector. The gas was contained in a cell with a 12 cm path length and equipped with polyethylene windows. Normally 256 scans at a resolution of 0.5 cm^{-1} were used to give a satisfactory signal-to-noise ratio.

The observed wavenumbers for the fundamentals of the trans-gauche (C_1) and gauche-gauche (C_2) conformers are listed in Tables 1 and 2, respectively, along with their predicted values. The predicted wavenumbers for the fundamentals of the least stable gauche-gauche' (C_s) conformer along with two tentative assignments are listed in Table 3.

Ab Initio Calculations

The LCAO-MO-SCF restricted Hartree-Fock (RHF) calculations were performed with the Gaussian-03 program²⁵ using Gaussian-type basis functions. The energy minima with respect to nuclear coordinates were obtained by simultaneous relaxation of all geometric parameters consistent with the symmetry restrictions using the gradient method of Pulay.²⁶ A number of basis sets starting from 6-31G(d) and increasing to 6-311+G-(2df,2pd) were employed at the level of restricted Hartree-Fock and/or Møller-Plesset perturbation theory to the second order (MP2) to obtain energy differences between the three stable conformers (Table 4). Density functional theory calculations were also carried out by the B3LYP method using the same basis sets. From the MP2 calculations with relatively large basis sets beginning with 6-311G(d,p), the trans-gauche rotamers are predicted to be the most stable, ranging in energy from 83 to 141 cm^{-1} lower than the second most stable gauche-gauche (C_2) conformer. The gauche-gauche' (C_s) rotamer is predicted to be the least stable, on the average by about 350 cm^{-1} with a high value of 403 cm^{-1} and a low of 271 cm^{-1} . The restricted Hartree-Fock calculations predict the gauche-gauche (C_2) form to be the most stable with the other two conformers having similar energies. Similarly the density functional calculations with all the basis sets except the 6-31G(d) predict the gauche-gauche (C_2) rotamer to be the most stable conformer with the trans-gauche form the next most stable conformer (Table 4). The determined structural parameters from some of these calculations are listed in Table 5. These results indicate that the theoretical predictions cannot be relied on to provide the correct conformer stability when the energy differences are about 200 cm^{-1} ($2.39\text{ kJ}\cdot\text{mol}^{-1}$) or less. Therefore, one must rely on the experimental determination for establishing the conformational stability order for 1,1-dicyclopropylethene.

To obtain a more complete description of the nuclear motions involved in the vibrational fundamentals of 1,1-dicyclopropylethene, we have carried out normal coordinate analysis. The force fields in Cartesian coordinates were calculated by the Gaussian-03 program²⁵ at the MP2/6-31G(d) level. The internal coordinates used to calculate the **G** and **B** matrices are listed along with the structural parameters in Table 5 and the numbering is shown in Figure 1. By using the **B** matrix²⁷ the force field in Cartesian coordinates was converted to a force field in internal coordinates (Table 1S), and the pure ab initio vibrational frequencies were reproduced. Subsequently, scaling factors of 0.88 for the CH stretches and 0.90 for all other modes were used along with the geometric average of scaling factors for interaction force constants to obtain the fixed scaled force field and the resultant wavenumbers. A set of symmetry coordinates was used (Table 2S) to determine the corresponding potential energy distributions (PEDs). A comparison between the observed and calculated wavenumbers of the three stable conformers of 1,1-dicyclopropylethene along with the calculated infrared intensities, Raman activities, depolarization ratios, and PEDs are given in Tables 1, 2, and 3.

To identify the fundamental vibrations for 1,1-dicyclopropylethene from the three possible conformers, the infrared spectra were predicted using fixed scaled frequencies and infrared intensities determined from the Gaussian-03 program²⁵ from MP2/6-31G(d) calculations. Infrared intensities were calculated based on the dipole moment derivatives with respect to Cartesian coordinates. The derivatives were taken from the ab initio calculations at the MP2/6-31G(d) level and transformed to normal coordinates by $(\partial\mu_w/\partial Q_i) = \sum_j (\partial\mu_w/\partial X_j) L_{ij}$, where Q_i is the i th normal coordinate, X_j is the j th Cartesian displacement

TABLE 1: Observed and Calculated^a Frequencies (cm⁻¹) for 1,1-Dicyclopropylethene Trans-Gauche (C₁)

vib no.	fundamental	ab initio	fixed scaled ^b	IR int.	Raman act.	dp ratio	IR gas ^c	IR Xe ^d	solid ^e	PED ^f	A ^g	B ^g	C ^g
<i>v</i> ₁	CH ₂ antisymmetric stretch	3314	3109	10.7	28.0	0.71	3097	3087	3087	46S ₁ , 41S ₂₉	77	13	10
<i>v</i> ₂	CH ₂ antisymmetric stretch	3299	3095	2.0	59.0	0.74	3088	3073	3068	52S ₂ , 35S ₃₀	79	20	1
<i>v</i> ₃	=CH ₂ symmetric stretch	3213	3014	8.7	19.4	0.48	3020	3005	3005	47S ₃ , 24S ₄ , 13S ₃₁	35	46	19
<i>v</i> ₄	CH ₂ symmetric stretch	3217	3018	1.1	374.1	0.06	3023	3012	3015	53S ₄ , 23S ₃	88	11	1
<i>v</i> ₅	CH ₂ symmetric stretch	3202	3004	8.6	65.2	0.21	3004	2992	2993	43S ₅ , 20S ₃₂ , 13S ₃₁ , 11S ₆	18	71	11
<i>v</i> ₆	CH stretch	3199	3001	4.3	16.3	0.65	3002	2992	2993	38S ₆ , 32S ₃₃ , 13S ₄ , 13S ₃₂	18	1	81
<i>v</i> ₇	C=C stretch	1720	1632	12.4	18.8	0.11	1636	1634	1630	67S ₇ , 15S ₁₀	10	90	0
<i>v</i> ₈	CH ₂ deformation	1563	1483	0.7	8.9	0.48	1457	1458	1452	82S ₈ , 14S ₁₂	50	49	1
<i>v</i> ₉	CH ₂ deformation	1523	1445	4.1	11.7	0.69	1437	1430	1428	88S ₉ , 11S ₃₅	8	28	63
<i>v</i> ₁₀	=CH ₂ deformation	1504	1427	2.2	21.5	0.23	1400	1400	1400	65S ₁₀	17	62	21
<i>v</i> ₁₁	CH in-plane bend	1409	1336	0.2	7.6	0.55	1337	1330	1331	43S ₁₁ , 15S ₁₀	60	8	32
<i>v</i> ₁₂	ring breathing	1268	1203	0.4	23.9	0.14	~1189	1198	1202	40S ₁₂ , 22S ₃₈ , 11S ₁₁	43	53	4
<i>v</i> ₁₃	CH ₂ twist	1242	1178	2.2	3.4	0.73	1177	1174	1173	45S ₁₃ , 44S ₂₀	15	26	59
<i>v</i> ₁₄	CH out-of-plane bend	1174	1114	2.3	1.3	0.69	1097	1101	1108	63S ₁₄ , 29S ₁₃	8	13	79
<i>v</i> ₁₅	CH ₂ twist	1150	1091	1.2	4.2	0.75	1097	1094	1095	25S ₁₅ , 16S ₂₁ , 15S ₁₁	78	22	0
<i>v</i> ₁₆	CH ₂ wag	1113	1056	4.6	0.6	0.45	1059	1051	1049	58S ₁₆ , 25S ₄₂ , 13S ₄₃	12	19	69
<i>v</i> ₁₇	CH ₂ wag	1104	1047	6.3	1.7	0.31	1027	1023	1021	52S ₁₇ , 17S ₄₃	37	47	16
<i>v</i> ₁₈	ring deformation	971	921	6.1	12.7	0.75	909	906	903	45S ₁₈ , 14S ₄₅	50	22	28
<i>v</i> ₁₉	ring deformation	991	941	18.8	5.8	0.69	925	924	921	70S ₁₉ , 13S ₂₃	2	95	3
<i>v</i> ₂₀	CH ₂ rock	869	825	6.3	6.4	0.73	825	823	824	25S ₂₀ , 32S ₁₈ , 14S ₁₄ , 12S ₁₃	36	36	28
<i>v</i> ₂₁	CH ₂ rock	832	789	0.2	1.2	0.59	793	794	790	61S ₂₁ , 16S ₁₅	0	51	49
<i>v</i> ₂₂	=CH ₂ twist	745	707	0.2	4.3	0.72	727	723	719	66S ₂₂	10	3	87
<i>v</i> ₂₃	CC(=C)C symmetric stretch	713	677	0.6	7.6	0.15	690	685	692	28S ₂₃ , 15S ₂₂ , 13S ₁₉ , 11S ₁₅	49	12	39
<i>v</i> ₂₄	ring-C out-of-plane bend	183	174	0.5	0.8	0.67	191		201	26S ₂₄ , 41S ₂₆ , 13S ₂₅ , 11S ₅₃	3	75	22
<i>v</i> ₂₅	ring-C in-plane bend	321	305	0.2	0.8	0.35	311		337*	34S ₂₅ , 27S ₅₂ , 20S ₅₁	64	25	11
<i>v</i> ₂₆	CC(=C)C bend	523	496	0.7	4.3	0.74	504	504	498	27S ₂₆ , 24S ₅₀	31	11	58
<i>v</i> ₂₇	torsion	57	54	0.03	0.3	0.74	65		84*	94S ₂₇	3	20	77
<i>v</i> ₂₈	=CH ₂ antisymmetric stretch	3304	3100	19.7	27.5	0.69	3093	3084	3079	65S ₂₈ , 17S ₂₉ , 15S ₁	53	25	22
<i>v</i> ₂₉	CH ₂ antisymmetric stretch	3309	3104	4.8	61.0	0.74	3096	3087	3087	31S ₂₉ , 33S ₂₈ , 26S ₁	30	30	40
<i>v</i> ₃₀	CH ₂ antisymmetric stretch	3293	3089	1.3	67.2	0.75		3073	3068	52S ₃₀ , 37S ₂	3	85	12
<i>v</i> ₃₁	CH ₂ symmetric stretch	3216	3017	11.8	19.6	0.56	3023	3012	3015	57S ₃₁ , 25S ₃ , 14S ₅	60	35	5
<i>v</i> ₃₂	CH ₂ symmetric stretch	3211	3012	15.0	45.3	0.54	3014	3005	3005	55S ₃₂ , 33S ₅	14	1	85
<i>v</i> ₃₃	CH stretch	3204	3006	8.3	21.7	0.74	3004	2992	2993	55S ₃₃ , 35S ₆	14	73	13
<i>v</i> ₃₄	CH ₂ deformation	1569	1488	2.2	10.2	0.73	1465	1463	1472	78S ₃₄ , 14S ₃₈	18	38	44
<i>v</i> ₃₅	CH ₂ deformation	1522	1444	1.4	5.4	0.71	1433	1426	1424	88S ₃₅	73	24	3
<i>v</i> ₃₆	CC(=C)C antisymmetric stretch	1472	1396	7.6	12.9	0.74	1400	1394	1392	33S ₃₆ , 21S ₃₇ , 12S ₃₄	80	18	2
<i>v</i> ₃₇	CH in-plane bend	1324	1256	11.2	14.0	0.36	1260	1257	1256	51S ₃₇ , 19S ₃₆ , 12S ₄₄	96	0	4
<i>v</i> ₃₈	ring breathing	1266	1201	0.4	11.8	0.18	1189	1192	1189	37S ₃₈ , 21S ₁₂	15	84	1
<i>v</i> ₃₉	CH ₂ twist	1238	1174	0.6	11.3	0.74	1177	1174	1173	42S ₃₉ , 46S ₄₈ , 11S ₄₀	75	20	5
<i>v</i> ₄₀	CH out-of-plane bend	1176	1115	1.6	2.3	0.71	1097	1101	1108	61S ₄₀ , 31S ₃₉	79	21	0
<i>v</i> ₄₁	CH ₂ twist	1117	1060	5.2	2.9	0.70	1066	1062	1058	17S ₄₁ , 20S ₄₄ , 16S ₁₇ , 11S ₄₉	77	23	0
<i>v</i> ₄₂	CH ₂ wag	1108	1051	1.8	0.5	0.65	1048	1044	1042	45S ₄₂ , 31S ₁₆ , 13S ₁₇	68	3	29
<i>v</i> ₄₃	CH ₂ wag	1097	1041	13.2	0.7	0.59	1023	1019	1008	62S ₄₃ , 18S ₄₂ , 10S ₁₇	72	1	27
<i>v</i> ₄₄	=CH ₂ wag	1020	968	17.4	8.1	0.74	957	961	959	29S ₄₄ , 37S ₄₇ , 15S ₃₆	73	20	7
<i>v</i> ₄₅	ring deformation	957	908	4.7	8.7	0.75	884	886	890	42S ₄₅	40	6	54
<i>v</i> ₄₆	=CH ₂ rock	897	851	48.1	1.2	0.74	879	874	876	77S ₄₆	3	7	90
<i>v</i> ₄₇	ring deformation	890	844	3.6	4.9	0.75	~843	843	842	27S ₄₇ , 21S ₄₆ , 14S ₄₉ , 12S ₄₄	9	30	61
<i>v</i> ₄₈	CH ₂ rock	866	822	4.1	4.1	0.73	818	815	818	27S ₄₈ , 31S ₄₅ , 16S ₄₀ , 14S ₃₉	51	10	39
<i>v</i> ₄₉	CH ₂ rock	808	766	1.7	4.9	0.75	773	773	773	37S ₄₉ , 33S ₄₁	88	8	4
<i>v</i> ₅₀	ring-C in-plane bend	228	216	0.6	2.4	0.73	223		233	35S ₅₀ , 34S ₅₃ , 14S ₂₄ , 12S ₂₆	13	9	78
<i>v</i> ₅₁	C=C in-plane bend	425	403	2.1	3.7	0.42	426	424	427	54S ₅₁ , 14S ₂₅	88	11	1
<i>v</i> ₅₂	ring-C out-of-plane bend	312	296	0.8	2.0	0.64	311		315	42S ₅₂ , 20S ₅₀ , 13S ₂₄ , 11S ₂₅	67	1	32
<i>v</i> ₅₃	C=C out-of-plane bend	633	600	3.8	3.3	0.27	635	632	635	39S ₅₃ , 18S ₂₄	14	8	78
<i>v</i> ₅₄	torsion	96	91	0.1	1.2	0.74	93		107	100S ₅₄	0	99	1

^a All ab initio frequencies, infrared intensities (km/mol), Raman activities (Å⁴/u), depolarization ratios, and percentage potential energy distributions are calculated at the MP2(full)/6-31G(d) level with valence electron correlation. ^b Scaled frequencies with scaling factors of 0.88 for CH stretches and 0.90 for all other modes. ^c Infrared spectrum of the gas recorded at 25 °C. ^d Infrared spectrum of the xenon solution recorded at -70 °C. ^e Infrared spectrum of the annealed solid, except those with an asterisk, which are from the Raman spectrum. ^f Symmetry coordinates with PED contribution less than 10% are omitted. ^g Values refer to percentage of A-, B-, and C-type infrared band contour composition.

coordinate, and L_{ij} is the transformation matrix between the Cartesian displacement coordinates and normal coordinates. The infrared intensities were then calculated by $(N\pi)/(3c^2)[(\partial\mu_x/\partial Q_i)^2 + (\partial\mu_y/\partial Q_i)^2 + (\partial\mu_z/\partial Q_i)^2]$. In Figure 3, parts E, D, and C, the simulated infrared spectra of the trans-gauche (C₁), gauche-gauche (C₂), and gauche-gauche' (C₃) conformers, respectively, are shown. The simulated spectra, calculated at -70 °C, of the mixture of three conformers with the ΔH between the first two conformers obtained from the variable-temperature study in xenon solutions, along with the predicted ΔE for the C₃

conformer, is shown in Figure 3B. It should be compared to the experimental spectrum of the xenon solution at -70 °C (Figure 3A). The predicted spectrum is in remarkable resemblance to the experimental spectrum, and the scaled predicted data were proven to be very useful in distinguishing the fundamentals for the three conformers.

Conformational Stability

To obtain reliable enthalpy differences among the conformers, it is important to choose well-defined bands that are relatively

TABLE 2: Observed and Calculated^a Frequencies (cm⁻¹) for 1,1-dicyclopropylethene Gauche-Gauche (C₂)

block	vib no.	fundamental	ab initio	fixed scaled ^b	IR int.	Raman act.	dp ratio	IR gas ^{c,h}	IR Xe ^{d,h}	PED ^f	A ^g	B ^g	C ^g
A	ν_1	CH ₂ antisymmetric stretch	3305	3101	12.5	42.5	0.60	3097		94S ₁	—	100	—
A	ν_2	CH ₂ antisymmetric stretch	3292	3089	2.3	129.2	0.74			94S ₂	—	100	—
A	ν_3	=CH ₂ symmetric stretch	3220	3021	4.2	160.8	0.09			92S ₃	—	100	—
A	ν_4	CH ₂ symmetric stretch	3212	3013	0.02	165.4	0.04			70S ₄ , 20S ₅	—	100	—
A	ν_5	CH ₂ symmetric stretch	3202	3004	13.6	117.1	0.12	3005		74S ₅ , 19S ₄	—	100	—
A	ν_6	CH stretch	3196	2998	4.3	22.0	0.24			91S ₆	—	100	—
A	ν_7	C=C stretch	1730	1641	9.0	11.1	0.07		1645	69S ₇ , 14S ₁₀	—	100	—
A	ν_8	CH ₂ deformation	1567	1487	0.6	2.6	0.27			81S ₈ , 15S ₁₂	—	100	—
A	ν_9	CH ₂ deformation	1522	1443	3.0	9.9	0.73			99S ₉	—	100	—
A	ν_{10}	=CH ₂ deformation	1488	1412	4.8	20.7	0.21			76S ₁₀	—	100	—
A	ν_{11}	CH in-plane bend	1424	1351	0.6	10.2	0.21	1348*	1345	52S ₁₁ , 13S ₁₂ , 11S ₈	—	100	—
A	ν_{12}	ring breathing	1268	1203	0.1	27.3	0.07			56S ₁₂ , 17S ₁₁ , 10S ₁₅	—	100	—
A	ν_{13}	CH ₂ twist	1238	1174	1.5	15.3	0.71			42S ₁₃ , 45S ₂₀ , 11S ₁₄	—	100	—
A	ν_{14}	CH out-of-plane bend	1174	1114	1.0	3.5	0.41			63S ₁₄ , 33S ₁₃	—	100	—
A	ν_{15}	CH ₂ twist	1144	1085	0.0006	7.2	0.75			33S ₁₅ , 23S ₁₁ , 21S ₂₁	—	100	—
A	ν_{16}	CH ₂ wag	1111	1054	1.1	0.4	0.45			79S ₁₆ , 18S ₁₇	—	100	—
A	ν_{17}	CH ₂ wag	1099	1042	3.4	0.4	0.69			72S ₁₇ , 20S ₁₆	—	100	—
A	ν_{18}	ring deformation	1000	949	1.0	9.0	0.65			36S ₁₈ , 28S ₁₉	—	100	—
A	ν_{19}	ring deformation	979	929	0.0009	15.2	0.73			40S ₁₉ , 24S ₁₈	—	100	—
A	ν_{20}	CH ₂ rock	875	830	9.5	6.3	0.71	833	829	30S ₂₀ , 30S ₁₈ , 16S ₁₄ , 15S ₁₃	—	100	—
A	ν_{21}	CH ₂ rock	836	793	0.2	1.0	0.47	795	799	69S ₂₁ , 11S ₁₅	—	100	—
A	ν_{22}	=CH ₂ twist	768	729	0.3	5.8	0.71			43S ₂₂ , 29S ₁₅ , 12S ₂₃	—	100	—
A	ν_{23}	CC(=C)C symmetric stretch	720	684	0.1	7.8	0.06	707	700*	19S ₂₃ , 34S ₂₂ , 14S ₁₉	—	100	—
A	ν_{24}	ring-C out-of-plane bend	449	426	0.2	3.8	0.65			37S ₂₄ , 27S ₂₆ , 12S ₂₃	—	100	—
A	ν_{25}	ring-C in-plane bend	289	274	0.02	2.4	0.26	290*		85S ₂₅	—	100	—
A	ν_{26}	CC(=C)C bend	179	169	0.2	0.4	0.73	185		51S ₂₆ , 47S ₂₄	—	100	—
A	ν_{27}	torsion	66	63	0.1	0.4	0.71			99S ₂₇	—	100	—
B	ν_{28}	=CH ₂ antisymmetric stretch	3310	3105	5.0	66.1	0.75			82S ₂₈ , 16S ₂₉	98	—	2
B	ν_{29}	CH ₂ antisymmetric stretch	3304	3100	20.4	11.5	0.75	3089		79S ₂₉ , 18S ₂₈	52	—	48
B	ν_{30}	CH ₂ antisymmetric stretch	3292	3088	0.1	6.4	0.75			94S ₃₀	86	—	14
B	ν_{31}	CH ₂ symmetric stretch	3213	3014	13.0	16.2	0.75	3019		73S ₃₁ , 24S ₃₂	89	—	11
B	ν_{32}	CH ₂ symmetric stretch	3202	3004	8.5	21.0	0.75			76S ₃₂ , 22S ₃₁	0	—	100
B	ν_{33}	CH stretch	3195	2998	11.1	43.9	0.75			95S ₃₃	20	—	80
B	ν_{34}	CH ₂ deformation	1566	1486	0.8	12.8	0.75			78S ₃₄ , 16S ₃₈	6	—	94
B	ν_{35}	CH ₂ deformation	1522	1444	2.4	8.5	0.75			100S ₃₅	35	—	65
B	ν_{36}	CC(=C)C antisymmetric stretch	1479	1403	4.7	9.7	0.75		1400	30S ₃₆ , 30S ₃₇ , 16S ₃₄	100	—	0
B	ν_{37}	CH in-plane bend	1286	1220	15.3	2.3	0.75	1220	1217	52S ₃₇ , 16S ₃₈ , 13S ₃₆	94	—	6
B	ν_{38}	ring breathing	1242	1178	3.3	3.8	0.75	1169	1163	30S ₃₈ , 18S ₄₈ , 14S ₃₉	70	—	30
B	ν_{39}	CH ₂ twist	1234	1171	2.5	1.6	0.75			30S ₃₉ , 28S ₄₈ , 16S ₃₈	91	—	9
B	ν_{40}	CH out-of-plane bend	1171	1111	1.8	3.3	0.75			63S ₄₀ , 32S ₃₉	1	—	99
B	ν_{41}	CH ₂ twist	1147	1088	15.1	2.6	0.75	(1097)	(1094)	31S ₄₁ , 18S ₄₄ , 18S ₄₉ , 10S ₃₇	99	—	1
B	ν_{42}	CH ₂ wag	1111	1054	7.3	0.1	0.75	1054	1049	81S ₄₂ , 17S ₄₃	27	—	73
B	ν_{43}	CH ₂ wag	1096	1040	14.8	0.1	0.75	(1023)	(1019)	77S ₄₃ , 17S ₄₂	81	—	19
B	ν_{44}	=CH ₂ wag	1009	958	15.4	1.7	0.75	947	951	32S ₄₄ , 37S ₄₇ , 16S ₃₆	93	—	7
B	ν_{45}	ring deformation	960	910	6.1	18.5	0.75			71S ₄₅	43	—	57
B	ν_{46}	=CH ₂ rock	915	868	45.9	0.1	0.75	(884)	(886)	99S ₄₆	17	—	83
B	ν_{47}	ring deformation	879	834	6.0	0.9	0.75	834	829	27S ₄₇ , 16S ₄₅ , 11S ₄₉	6	—	94
B	ν_{48}	CH ₂ rock	855	811	4.3	0.8	0.75	814		23S ₄₈ , 19S ₄₉ , 14S ₄₀ , 12S ₃₉ , 11S ₄₇	85	—	15
B	ν_{49}	CH ₂ rock	817	775	2.8	4.4	0.75			43S ₄₉ , 30S ₄₁ , 14S ₄₇	86	—	14
B	ν_{50}	ring-C in-plane bend	648	615	8.8	3.1	0.75	619	620	32S ₅₀ , 41S ₅₃ , 12S ₄₁	32	—	68
B	ν_{51}	C=C in-plane bend	488	454	2.0	1.5	0.75	476	477	44S ₅₁ , 23S ₅₂	91	—	9
B	ν_{52}	ring-C out-of-plane bend	320	304	0.5	0.3	0.75			34S ₅₂ , 37S ₅₁ , 22S ₅₀	74	—	26
B	ν_{53}	C=C out-of-plane bend	200	189	0.9	2.2	0.75			44S ₅₃ , 28S ₅₂ , 25S ₅₀	36	—	64
B	ν_{54}	torsion	66	63	0.03	0.4	0.75			97S ₅₄	58	—	42

^a All ab initio frequencies, infrared intensities (km/mol), Raman activities ($\text{\AA}^4/\text{u}$), depolarization ratios, and percentage potential energy distributions are calculated at the MP2/6-31G(d) level with full electron correlation. ^b Scaled frequencies with scaling factors of 0.88 for CH stretches and 0.90 for all other modes. ^c Infrared spectrum of the gas recorded at 25 °C; bands with asterisks are from the Raman spectrum of the liquid. ^d Infrared spectrum of the xenon solution recorded at -70 °C. ^e Symmetry coordinates with PED contribution less than 10% are omitted. ^f Values refer to percentage of A-, B-, and C-type infrared band contour composition; entries with a dash are symmetry forbidden. ^h Observed wavenumbers in parentheses overlap trans-gauche (C₁) bands.

isolated and arise from a single conformer, along with correct assignments. By comparison of the infrared spectrum of the xenon solutions with the infrared spectrum of the annealed solid, several bands can be identified as due to a less stable conformer in the fluid phases. However, it should be noted that the most stable conformer in the solid may not be the most stable one in the fluid states due to packing factors and dipole interactions. The most pronounced band to disappear is the 1217 cm⁻¹ band

(Figure 2), which is well-separated with appropriate intensity for ΔH determinations. Similarly the pronounced bands at 1163, 951, 829, and 477 cm⁻¹ are not present in the spectrum of the solid (Figure 2). The pair at 1257 and 1217 cm⁻¹ in the xenon solution are predicted at 1256 (intensity 11.2 km³mol⁻¹) and 1220 (intensity 15.3 km³mol⁻¹) cm⁻¹ for the trans-gauche (C₁) and gauche-gauche (C₂) conformers, respectively, which clearly shows that the trans-gauche (C₁) rotamer is the one present in

TABLE 3: Observed and Calculated^a Frequencies (cm⁻¹) for 1,1-Dicyclopropylethene *Gauche-Gauche'* (C_s)

block	vib no.	fundamental	ab initio	fixed scaled ^b	IR int.	Raman act.	dp ratio	IR gas ^c	IR Xe ^{d,h}	PED ^f	A ^g	B ^g	C ^g
A'	ν_1	CH ₂ antisymmetric stretch	3307	3102	20.0	39.6	0.57		99S ₁		—	29	71
A''	ν_2	CH ₂ antisymmetric stretch	3293	3089	0.04	39.0	0.75		97S ₂		100	—	—
A'	ν_3	=CH ₂ symmetric stretch	3222	3023	4.4	147.2	0.09		94S ₃		—	94	6
A'	ν_4	CH ₂ symmetric stretch	3212	3013	0.6	210.6	0.02		87S ₄		—	75	25
A''	ν_5	CH ₂ symmetric stretch	3204	3006	1.2	19.3	0.75		83S ₅ , 17S ₃₁		100	—	—
A'	ν_6	CH stretch	3190	2992	21.2	112.9	0.39		98S ₆		—	6	94
A'	ν_7	C=C stretch	1730	1641	9.9	10.1	0.07		69S ₇ , 15S ₁₀		—	99	1
A'	ν_8	CH ₂ deformation	1569	1489	2.8	4.5	0.44		81S ₈ , 15S ₁₂		—	3	97
A''	ν_9	CH ₂ deformation	1521	1443	1.4	4.3	0.75		100S ₉		100	—	—
A'	ν_{10}	=CH ₂ deformation	1489	1413	5.5	22.3	0.24		75S ₁₀		—	54	46
A'	ν_{11}	CH in-plane bend	1436	1362	0.7	14.1	0.35		56S ₁₁ , 12S ₈ , 11S ₁₂		—	94	6
A'	ν_{12}	Ring breathing	1273	1207	0.4	25.5	0.04		59S ₁₂ , 16S ₁₁		—	77	23
A''	ν_{13}	CH ₂ twist	1236	1172	1.1	4.9	0.75		33S ₁₃ , 37S ₂₀		100	—	—
A''	ν_{14}	CH out-of-plane bend	1167	1107	0.008	2.7	0.75		62S ₁₄ , 33S ₁₃		100	—	—
A'	ν_{15}	CH ₂ twist	1164	1105	0.1	9.0	0.74		33S ₁₅ , 20S ₂₁ , 18S ₁₁		—	43	57
A''	ν_{16}	CH ₂ wag	1110	1053	0.8	0.2	0.75		74S ₁₆ , 23S ₄₃		100	—	—
A'	ν_{17}	CH ₂ wag	1104	1047	9.6	0.6	0.67		69S ₁₇ , 24S ₄₂		—	3	97
A''	ν_{18}	ring deformation	960	911	6.2	13.5	0.75		68S ₁₈		100	—	—
A'	ν_{19}	Ring deformation	983	933	3.9	4.1	0.64		49S ₁₉ , 19S ₄₅		—	21	79
A''	ν_{20}	CH ₂ rock	852	808	4.6	1.3	0.75		23S ₂₀ , 20S ₄₉ , 15S ₁₄ , 12S ₄₇ , 12S ₁₃		100	—	—
A'	ν_{21}	CH ₂ rock	837	794	0.2	0.8	0.16		73S ₂₁ , 10S ₁₅		—	81	19
A''	ν_{22}	=CH ₂ twist	739	701	1.1	1.0	0.75		80S ₂₂		100	—	—
A'	ν_{23}	CC(=C)C symmetric stretch	749	710	0.3	8.9	0.36		25S ₂₃ , 35S ₁₅ , 11S ₁₉		—	100	0
A''	ν_{24}	ring-C out-of-plane bend	322	306	0.1	0.2	0.75		42S ₂₄ , 35S ₅₁ , 18S ₅₀		100	—	—
A'	ν_{25}	ring-C in-plane bend	230	218	0.2	2.4	0.48		49S ₂₅ , 28S ₅₃ , 18S ₂₆		—	58	42
A'	ν_{26}	CC(=C)C bend	422	400	2.2	4.9	0.50	415?	418?	24S ₂₆ , 20S ₅₂ , 20S ₂₃	—	36	64
A''	ν_{27}	torsion	34	32	0.02	0.1	0.75		99S ₂₇		100	—	—
A''	ν_{28}	=CH ₂ antisymmetric stretch	3311	3106	5.0	62.4	0.75		88S ₂₈ , 11S ₂₉		100	—	—
A''	ν_{29}	CH ₂ antisymmetric stretch	3304	3100	17.0	9.8	0.75		87S ₂₉ , 12S ₂₈		100	—	—
A'	ν_{30}	CH ₂ antisymmetric stretch	3295	3091	0.5	94.8	0.75		99S ₃₀		—	100	0
A''	ν_{31}	CH ₂ symmetric stretch	3212	3013	12.2	22.5	0.75		81S ₃₁ , 17S ₅		100	—	—
A'	ν_{32}	CH ₂ symmetric stretch	3206	3007	19.5	55.1	0.26		91S ₃₂		—	94	6
A''	ν_{33}	CH stretch	3186	2989	0.1	0.9	0.75		98S ₃₃		100	—	—
A''	ν_{34}	CH ₂ deformation	1566	1486	0.02	11.8	0.75		77S ₃₄ , 16S ₃₈		100	—	—
A'	ν_{35}	CH ₂ deformation	1524	1446	3.8	12.0	0.71		98S ₃₅		—	100	0
A''	ν_{36}	CC(=C)C antisymmetric stretch	1478	1402	3.3	3.7	0.75		31S ₃₆ , 28S ₃₇ , 16S ₃₄		100	—	—
A''	ν_{37}	CH in-plane bend	1280	1215	12.0	7.0	0.75		48S ₃₇ , 21S ₃₈		100	—	—
A''	ν_{38}	ring breathing	1228	1165	6.1	2.3	0.75		34S ₃₈ , 15S ₄₄ , 10S ₃₆		100	—	—
A'	ν_{39}	CH ₂ twist	1239	1175	2.9	11.1	0.74		43S ₃₉ , 45S ₄₈ , 11S ₄₀		—	81	19
A'	ν_{40}	CH out-of-plane bend	1174	1113	3.3	4.2	0.51		64S ₄₀ , 32S ₃₉		—	76	24
A''	ν_{41}	CH ₂ twist	1136	1078	9.4	0.5	0.75		33S ₄₁ , 21S ₄₉ , 15S ₃₇ , 14S ₄₄		100	—	—
A'	ν_{42}	CH ₂ wag	1111	1054	9.5	0.4	0.51		75S ₄₂ , 22S ₁₇		—	49	51
A''	ν_{43}	CH ₂ wag	1091	1035	8.6	0.3	0.75		70S ₄₃ , 23S ₁₆		100	—	—
A''	ν_{44}	=CH ₂ wag	1008	956	12.8	5.4	0.75		32S ₄₄ , 36S ₄₇ , 16S ₃₆		100	—	—
A'	ν_{45}	ring deformation	1003	952	14.1	13.7	0.70		40S ₄₅ , 21S ₁₉		—	37	63
A'	ν_{46}	=CH ₂ rock	912	865	44.7	0.1	0.75	883?	(886)	98S ₄₆	—	25	75
A''	ν_{47}	ring deformation	883	838	0.02	5.9	0.75		25S ₄₇ , 19S ₁₈		100	—	—
A'	ν_{48}	CH ₂ rock	872	827	11.3	6.7	0.73		30S ₄₈ , 29S ₄₅ , 18S ₄₀ , 16S ₃₉		—	100	0
A''	ν_{49}	CH ₂ rock	809	768	1.1	5.0	0.75		42S ₄₉ , 33S ₄₁ , 12S ₄₇		100	—	—
A''	ν_{50}	ring-C in-plane bend	297	282	0.2	1.8	0.75		48S ₅₀ , 38S ₂₄		100	—	—
A''	ν_{51}	C=C in-plane bend	503	477	0.7	1.3	0.75		45S ₅₁ , 25S ₅₀		100	—	—
A'	ν_{52}	ring-C out-of-plane bend	164	156	0.8	0.6	0.68		48S ₅₂ , 35S ₂₆ , 19S ₅₃		—	92	8
A'	ν_{53}	C=C out-of-plane bend	626	594	5.9	3.4	0.28		38S ₅₃ , 15S ₅₂ , 12S ₂₅		—	4	96
A'	ν_{54}	torsion	71	68	0.2	0.5	0.69		100S ₅₄		—	99	1

^a All ab initio frequencies, infrared intensities (km/mol), Raman activities ($\text{\AA}^4/\text{u}$), depolarization ratios, and percentage potential energy distributions are calculated at the MP2/6-31G(d) level with full electron correlation. ^b Scaled frequencies with scaling factors of 0.88 for CH stretches and 0.90 for all other modes. ^c Infrared spectrum of the gas recorded at 25 °C. ^d Infrared spectrum of the xenon solution recorded at -70 °C. ^e Symmetry coordinates with PED contribution less than 10% are omitted. ^f Values refer to percentage of A-, B-, and C-type infrared band contour composition; entries with a dash are symmetry forbidden. ^g Observed wavenumbers in parentheses overlap trans-gauche (C₁) bands.

the crystalline solid. This conclusion is supported by the assignment of other disappearing bands such as the one at 476 cm⁻¹ with a predicted frequency of 454 cm⁻¹ for the gauche-gauche conformer, whereas the corresponding mode for the trans-gauche form is predicted at 496 cm⁻¹. The only band remaining in this region in the crystalline solid is observed at 498 cm⁻¹, again, clearly showing that the trans-gauche (C₁) form is the one present in the solid. This conclusion is also supported by the earlier reported Raman data where a line was reported at 1348 cm⁻¹ in the spectrum of the liquid but not present in

the spectrum of the solid. This line is confidently assigned to the gauche-gauche (C₂) conformer where it is predicted at 1351 cm⁻¹ with an activity of 10.2 $\text{\AA}^4/\text{u}$; the corresponding mode for the trans-gauche (C₁) form is predicted at 1336 cm⁻¹ (activity 7.6 $\text{\AA}^4/\text{u}$) and observed at 1337 cm⁻¹ in the infrared spectrum of the gas and at 1330 cm⁻¹ in the Raman spectrum of the liquid and this band remains in the Raman spectrum of the solid.

With confident assignments for the 1257 (C₁) and 1217 (C₂) cm⁻¹ bands we then used this pair initially to determine which conformer is the most stable rotamer in the xenon solutions.

TABLE 4: Calculated Energies and Energy Differences for the Three Conformers of 1,1-Dicyclopropylethene

method/basis set	trans-gauche	gauche-gauche	ΔE (cm ⁻¹)	gauche-gauche'	ΔE (cm ⁻¹)
RHF/6-31G(d)	-309.842281	-309.843461	-259	-309.842177	23
RHF/6-31+G(d)	-309.848349	-309.849599	-274	-309.848357	-2
MP2/6-31G(d)	-310.914974	-310.915014	-9	-310.913696	281
MP2/6-31+G(d)	-310.934053	-310.934278	-49	-310.932816	271
MP2/6-31G(d,p)	-311.014465	-311.014306	35	-311.013076	305
MP2/6-31+G(d,p)	-311.032249	-311.032261	-3	-311.030927	290
MP2/6-311G(d)	-311.134411	-311.134459	-11	-311.133058	297
MP2/6-311+G(d)	-311.141911	-311.141827	18	-311.140428	325
MP2/6-311G(d,p)	-311.226870	-311.226492	83	-311.225306	342
MP2/6-311+G(d,p)	-311.233969	-311.233620	77	-311.232395	345
MP2/6-311G(2d,2p)	-311.312606	-311.311946	145	-311.310772	403
MP2/6-311+G(2d,2p)	-311.317585	-311.316996	129	-311.315887	373
MP2/6-311G(2df,2pd)	-311.440500	-311.439864	140	-311.438742	386
MP2/6-311+G(2df,2pd)	-311.444409	-311.443766	141	-311.442738	367
B3LYP/6-31G(d)	-311.990387	-311.990285	23	-311.989072	289
B3LYP/6-31+G(d)	-312.001784	-312.001957	-38	-312.000786	219
B3LYP/6-311G(d,p)	-312.073410	-312.073757	-76	-312.072622	173
B3LYP/6-311+G(d,p)	-312.075833	-312.076150	-70	-312.075101	160
B3LYP/6-311G(2d,2p)	-312.086188	-312.086484	-65	-312.085360	182
B3LYP/6-311+G(2d,2p)	-312.088547	-312.088798	-55	-312.087794	165
B3LYP/6-311G(2df,2pd)	-312.096463	-312.096723	-57	-312.095634	182
B3LYP/6-311+G(2df,2pd)	-312.098600	-312.098812	-47	-312.097830	169

To obtain the enthalpy difference, spectral data were measured at five-degree intervals between -55 and -100 °C (Figure 4). These sets of intensity data were fit to the van't Hoff equation, $-\ln K = \Delta H/RT - \Delta S/R$, where K is the intensity ratio of C_1/C_2 , assuming that ΔH is not a function of temperature in the range of investigation. The value of 106 ± 5 cm⁻¹ (Table 6) obtained from this pair is expected to be the lower limit because the 1217 cm⁻¹ band clearly has at least one weak band near this frequency in the spectrum of the solid (Figure 2). Since both bands are very symmetric with good intensity along with well-defined baselines, the statistical uncertainty is very small. We then combined the 1217 cm⁻¹ band with the 1174 and 961 cm⁻¹ bands of the C_1 conformer to obtain additional enthalpy differences. We also used the 951 cm⁻¹ band of the gauche-gauche (C_2) conformer to obtain three more enthalpy differences. We tried the pair of bands at 632 and 620 cm⁻¹ but the latter one has such a poor signal-to-noise ratio (Figure 4), because of the absorption of the silicon windows, the results were unreliable. All of the meaningful results are listed in Table 6 and there are relatively large variations among the values. Such variations are expected because of the underlying combination and/or overtone bands present in this spectral region, particularly with so many low-frequency bending modes. Nevertheless, by using the average of six band pairs, it is hoped that their effect

will cancel out. By using a least-squares fit and the slopes of the van't Hoff plots, an average ΔH value of 146 ± 6 cm⁻¹ (1.75 ± 0.07 kJ·mol⁻¹) was obtained with the C_1 conformer the more stable form. The statistical uncertainty is quite low, although there is no doubt on the presence of interference of the measured bands from combinations and overtone bands. Thus, a more reasonable uncertainty is about 20% to provide a more realistic error value. The final value of 146 ± 30 cm⁻¹ (1.75 ± 0.36 kJ·mol⁻¹) is obtained for the enthalpy difference between the C_2 rotamer and the more stable C_1 conformer.

Vibrational Assignment

The vibrational assignment for the more stable C_1 conformer can be made rather straightforwardly based on the ab initio predicted frequencies, the predicted gas-phase band envelopes, and the Raman depolarization ratios. To aid the vibrational assignment we also predicted the Raman spectra for all three of the conformers. The calculated spectra were simulated from ab initio MP2(full)/6-31G(d) scaled frequencies and Raman scattering activities. The Raman scattering cross-sections, $\partial\sigma/\partial\Omega$, which are proportional to the Raman intensities, can be calculated from the scattering activities and the predicted frequencies for each normal mode.²⁸⁻³¹ To obtain the polarized Raman scattering cross sections, the polarizabilities are incorporated into S_j by multiplying S_j by $(1 - \rho_j)/(1 + \rho_j)$, where ρ_j is the depolarization ratio of the j th normal mode. The Raman scattering cross sections and calculated scaled frequencies were used together with a Lorentzian function to obtain the calculated spectrum. The predicted Raman spectra of the trans-gauche (C_1), gauche-gauche (C_2), and gauche-gauche' (C_3) conformers are shown in Figure 5, parts E, D, and C, respectively. The spectrum of the mixture of the three conformers utilizing the predicted ΔE for the C_3 form and the experimental ΔH value for the C_2 form, calculated at 25°C, is shown in Figure 5B; the experimental Raman spectrum of the liquid at ambient temperature is shown in Figure 5A. The agreement between the predicted and observed spectra is reasonably good but not nearly as good as the agreement of the simulated infrared spectrum due to the significantly stronger intermolecular interaction in the liquid phase. Nevertheless, these spectra were of considerable aid in making the vibrational assignment for the two most abundant conformers.

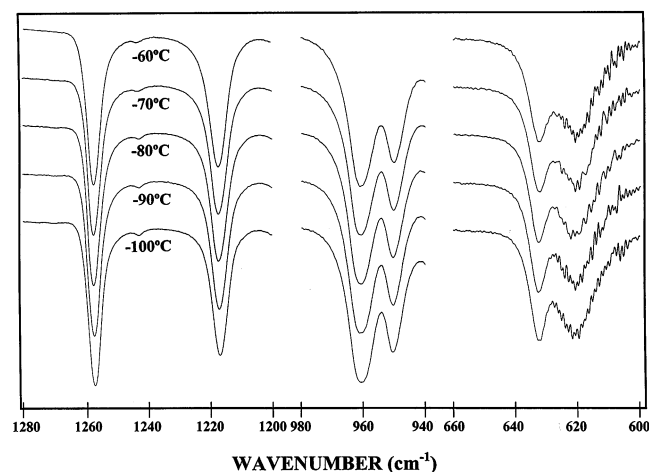


Figure 4. Infrared spectra of 1,1-dicyclopropylethene in xenon solution at different temperatures.

TABLE 5: Structural Parameters (Å and Degree), Rotational Constants (MHz), and Dipole Moments (D) for the Three Stable Rotamers of 1,1-Dicyclopropylethene

structural parameters	internal coord	MP2/6-311+G(d,p)			electron diffraction ^a			adjusted r_0		
		t_g (C_1)	gg (C_2)	gg' (C_3)	r_a t_g (C_1)	r_a gg (C_2)	r_a gg (C_2)	t_g (C_1)	gg (C_2)	gg' (C_3)
$r(C_1=C_2)$	R_1	1.348	1.345	1.345	1.331	1.3271	1.3205(30)	1.336	1.336	1.336
$r(C_1C_3)$	R_2	1.490	1.489	1.490	1.496	1.4960	1.4930(26)	1.490	1.489	1.490
$r(C_1C_4)$	R_3	1.486	1.489	1.490	1.494	1.4960	1.4930(26)	1.486	1.489	1.490
$r(C_3C_7)$	R_4	1.507	1.505	1.505	1.511	1.5120	1.4970(11)	1.508	1.506	1.506
$r(C_3C_8)$	R_5	1.518	1.517	1.516	1.511	1.5120	1.4970(11)	1.519	1.518	1.517
$r(C_7C_8)$	R_6	1.508	1.510	1.511	1.511	1.512	1.497(1)	1.511	1.513	1.514
$r(C_4C_9)$	R_7	1.516	1.505	1.505	1.511	1.5120	1.4970(11)	1.517	1.506	1.506
$r(C_4C_{10})$	R_8	1.517	1.517	1.516	1.511	1.5120	1.4970(11)	1.518	1.518	1.517
$r(C_9C_{10})$	R_9	1.505	1.510	1.511	1.511	1.512	1.497(1)	1.508	1.513	1.514
$r(C_2H_{19})$	r_1	1.084	1.085	1.085				1.084	1.085	1.085
$r(C_2H_{20})$	r_2	1.086	1.085	1.085				1.086	1.085	1.085
$r(C_3H_5)$	r_3	1.087	1.088	1.088		1.0931	1.0598(12)	1.087	1.088	1.088
$r(C_4H_6)$	r_4	1.087	1.088	1.088		1.0931	1.0598(12)	1.087	1.088	1.088
$r(C_7H_{11})$	r_5	1.083	1.083	1.083		1.0931	1.0598(12)	1.083	1.083	1.083
$r(C_8H_{13})$	r_7	1.085	1.084	1.084		1.0931	1.0598(12)	1.085	1.084	1.084
$r(C_7H_{12})$	r_6	1.084	1.084	1.084		1.0931	1.0598(12)	1.084	1.084	1.084
$r(C_8H_{14})$	r_8	1.084	1.084	1.084		1.0931	1.0598(12)	1.084	1.084	1.084
$r(C_9H_{15})$	r_9	1.083	1.083	1.083		1.0931	1.0598(12)	1.083	1.083	1.083
$r(C_{10}H_{17})$	r_{11}	1.083	1.085	1.084		1.0931	1.0598(12)	1.083	1.085	1.084
$r(C_9H_{16})$	r_{10}	1.084	1.084	1.084		1.0931	1.0598(12)	1.084	1.084	1.084
$r(C_{10}H_{18})$	r_{12}	1.084	1.084	1.084		1.0931	1.0598(12)	1.084	1.084	1.084
$\angle C_3C_1C_4$	λ	117.6	113.7	113.8				117.6	113.7	113.8
$\angle C_3C_1C_2$	κ_1	122.3	123.1	123.1			122.95(33)	122.3	123.1	123.1
$\angle C_4C_1C_2$	κ_2	120.1	123.1	123.1			122.95(33)	120.1	123.1	123.1
$\angle C_1C_3C_7$	μ_1	121.9	122.4	122.8				121.9	122.4	122.8
$\angle C_1C_3C_8$	μ_2	119.4	118.8	119.6				119.4	118.8	119.6
$\angle C_1C_4C_9$	ν_1	121.7	122.4	122.8				121.7	122.4	122.8
$\angle C_1C_4C_{10}$	ν_2	121.4	118.8	119.6				121.4	118.8	119.6
$\angle C_7C_3C_8$		59.8	59.6	60.0	60.0	60.0	60.0	59.8	59.6	60.0
$\angle C_3C_7C_8$		60.5	60.0	60.4	60.0	60.0	60.0	60.5	60.0	60.4
$\angle C_3C_8C_7$		59.7	60.4	59.6	60.0	60.0	60.0	59.7	60.4	59.6
$\angle C_9C_4C_{10}$		59.5	60.0	59.6	60.0	60.0	60.0	59.5	60.0	59.6
$\angle C_4C_9C_{10}$		60.3	60.4	60.4	60.0	60.0	60.0	60.3	60.4	60.4
$\angle C_4C_{10}C_9$		60.2	59.6	60.0	60.0	60.0	60.0	60.2	59.6	60.0
$\angle C_1C_2H_{19}$	σ_1	121.7	121.2	121.3			121.57	121.7	121.2	121.3
$\angle C_1C_2H_{20}$	σ_2	120.8	121.2	121.3			121.57	120.8	121.2	121.3
$\angle H_{19}C_2H_{20}$	ϕ	117.6	117.6	117.5				117.6	117.6	117.5
$\angle C_1C_3H_5$	ξ_1	115.2	114.3	114.1			114.11	115.2	114.3	114.1
$\angle C_7C_3H_5$	η_1	114.8	116.0	115.5				114.8	116.0	115.5
$\angle C_8C_3H_5$	η_2	114.5	114.5	114.3				114.5	114.5	114.3
$\angle C_1C_4H_6$	ζ_2	114.0	114.3	114.1			114.11	114.0	114.3	114.1
$\angle C_9C_4H_6$	θ_1	115.1	114.5	115.5				115.1	114.5	115.5
$\angle C_{10}C_4H_6$	θ_2	114.6	116.0	114.3				114.6	116.0	114.3
$\angle C_3C_7H_{11}$	α_1	118.1	117.9	118.0				118.1	117.9	118.0
$\angle C_3C_7H_{12}$	α_2	117.4	117.7	117.6				117.4	117.7	117.6
$\angle C_8C_7H_{11}$	α_3	117.1	117.0	117.0				117.1	117.0	117.0
$\angle C_8C_7H_{12}$	α_4	118.0	118.0	118.0				118.0	118.0	118.0
$\angle C_3C_8H_{13}$	β_1	116.2	116.5	116.5				116.2	116.5	116.5
$\angle C_3C_8H_{14}$	β_2	118.3	118.2	118.3				118.3	118.2	118.3
$\angle C_7C_8H_{13}$	β_3	116.9	116.8	116.9				116.9	116.8	116.9
$\angle C_7C_8H_{14}$	β_4	118.5	118.5	118.6				118.5	118.5	118.6
$\angle H_{11}C_7H_{12}$	ϵ_1	115.1	115.1	115.0			114.53	115.1	115.1	115.0
$\angle H_{13}C_8H_{14}$	ϵ_2	115.7	115.6	115.6			114.53	115.7	115.6	115.6
$\angle C_4C_9H_{15}$	γ_1	117.2	116.5	118.0				117.2	116.5	118.0
$\angle C_4C_9H_{16}$	γ_2	117.2	118.5	117.6				117.2	118.2	117.6
$\angle C_{10}C_9H_{15}$	γ_3	117.3	116.8	117.0				117.3	116.8	117.0
$\angle C_{10}C_9H_{16}$	γ_4	118.1	117.7	118.0				118.1	118.5	118.0
$\angle C_4C_{10}H_{17}$	δ_1	117.8	117.9	116.5				117.8	117.9	116.5
$\angle C_4C_{10}H_{18}$	δ_2	117.0	118.2	118.3				117.0	117.7	118.3
$\angle C_9C_{10}H_{17}$	δ_3	117.6	117.0	116.9				117.6	117.0	116.9
$\angle C_9C_{10}H_{18}$	δ_4	118.3	118.0	118.6				118.3	118.0	118.6
$\angle H_{15}C_9H_{16}$	ϵ_3	115.6	115.6	115.0			114.53	115.6	115.6	115.0
$\angle H_{17}C_{10}H_{18}$	ϵ_4	115.0	115.1	115.6			114.53	115.0	115.1	115.6
$\tau C_7C_3C_1C_2$	τ_1	-21.7	-23.9	-20.1				-21.7	-23.9	-20.1
$\tau C_8C_3C_1C_2$	τ_1	-92.5	-94.7	-91.5				-92.5	-94.7	-91.5
$\tau C_9C_4C_1C_2$	τ_2	147.4	-94.7	20.1				147.4	-94.7	20.1
$\tau C_{10}C_4C_1C_2$	τ_2	-141.5	-23.9	91.5				-141.5	-23.9	91.5
$\tau C_7C_3C_1H_5$		-147.0	-149.0	-148.0				-147.0	-149.0	-148.0
$\tau C_8C_3C_1H_5$		142.2	140.2	140.5				142.2	140.2	140.5
$\tau C_9C_4C_1H_6$		145.1	140.2	148.0				145.1	140.2	148.0

TABLE 5: (Continued)

structural parameters	internal coord	MP2/6-311+G(d,p)			electron diffraction ^a			adjusted r_0		
		$tg (C_1)$	$gg (C_2)$	$gg' (C_s)$	r_a $tg (C_1)$	r_a $gg (C_2)$	r_a $gg (C_2)$	$tg (C_1)$	$gg (C_2)$	$gg' (C_s)$
$\tau C_{10}C_4C_1H_6$		-143.7	-149.0	-140.5				-143.7	-149.0	-140.5
$\tau H_{11}C_7C_3C_1$		-1.0	-0.1	-1.0				-1.0	-0.1	-1.0
$\tau H_{13}C_8C_3C_1$		4.8	5.9	6.0				4.8	5.9	6.0
$\tau H_{12}C_7C_3C_1$		143.9	144.9	144.0				143.9	144.9	144.0
$\tau H_{14}C_8C_3C_1$		-139.8	-138.8	-138.7				-139.8	-138.8	-138.7
$\tau H_{15}C_9C_4C_1$		2.8	5.9	1.0				2.8	5.9	1.0
$\tau H_{17}C_{10}C_4C_1$		-3.2	-0.1	-6.0				-3.2	-0.1	-6.0
$\tau H_{16}C_9C_4C_1$		-141.2	-138.8	-144.0				-141.2	-138.8	-144.0
$\tau H_{18}C_{10}C_4C_1$		140.5	144.9	138.7				140.5	144.9	138.7
A		3329.2	4357.5	4048.7				3341.6	4374.0	4062.3
B		1601.1	1285.7	1397.2				1600.7	1285.0	1396.7
C		1255.1	1123.2	1165.2				1256.7	1124.0	1165.8
$ \mu_a $		0.188								
$ \mu_b $		0.616	0.557	0.554						
$ \mu_c $		0.069		0.219						
$ \mu_t $		0.648	0.557	0.596						

^a Reference 19. ^b Calculated from ref 19 results.TABLE 6: Temperature-Dependent Intensity Ratios for the Trans-Gauche (C_1) and Gauche-Gauche (C_2) Conformers of 1,1-Dicyclopromethylene Dissolved in Liquid Xenon

$T (^\circ C)$	$1000/T (K^{-1})$	I_{1257tg}/I_{1217gg}	I_{1174tg}/I_{1217gg}	I_{961tg}/I_{1217gg}	I_{1257tg}/I_{951gg}	I_{1174tg}/I_{951gg}	I_{961tg}/I_{951gg}
-55.0	4.5840	0.98473	0.57031	4.91597	0.50239	0.67921	2.50806
-60.0	4.6915	0.99214	0.59078	5.09798	0.50773	0.70482	2.60893
-65.0	4.8042	0.99260	0.61358	5.20813	0.51259	0.72554	2.68756
-70.0	4.9225	1.01785	0.63636	5.37213	0.52275	0.74834	2.75901
-75.0	5.0467	1.03760	0.66265	5.65126	0.52992	0.78055	2.88621
-80.0	5.1773	1.07395	0.68859	5.91121	0.53744	0.80140	2.95814
-85.0	5.3149	1.08426	0.71052	6.05760	0.54395	0.82576	3.03899
-90.0	5.4600	1.11548	0.73873	6.32796	0.55866	0.85980	3.16921
-95.0	5.6132	1.12893	0.76857	6.55676	0.56611	0.88918	3.28796
-100.0	5.7753	1.17388	0.80404	6.99177	0.57869	0.91953	3.44679
$\Delta H (cm^{-1})$	individual pair	106 ± 5	166 ± 4	202 ± 5	83 ± 2	143 ± 1	179 ± 4
$\Delta H (cm^{-1})$	statistical av				146 ± 6		

For the most stable trans-gauche conformer, we have listed the frequencies of the observed fundamentals in the gaseous, xenon solution, and solid phases (Table 1). In many cases the

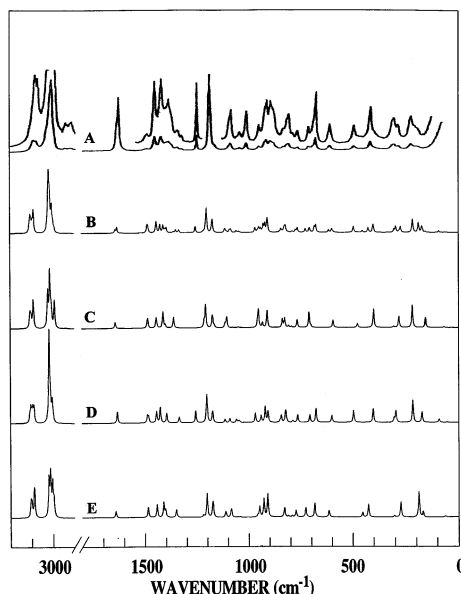


Figure 5. Raman spectra of 1,1-dicyclopromethylene: (A) liquid at 25 °C; (B) calculated spectrum of the mixture of three conformers with ΔH of 146 and 350 cm^{-1} ; (C) calculated spectrum of the gauche-gauche', C_s conformer; (D) calculated spectrum of the gauche-gauche, C_2 conformer; and (E) calculated spectrum of the trans-gauche conformer.

frequencies for the gas had to be estimated from the spectra of the xenon solutions since the vibrations for the two cyclopromyl rings are overlapped with additional contributions from the modes of the C_2 conformer (Figure 6). Additionally most of the fundamentals in both infrared and Raman spectra of crystalline solid are doublets with a few of them exhibiting some shifts which is an indication that there are two molecules per primitive cell. Only a few bands involve assignments that are difficult, or questionable, or differ significantly from those previously reported.¹⁶ Therefore only these latter vibrations will be discussed.

For many monosubstituted three-membered-ring molecules, the C-H stretch on the carbon with the substituent is between

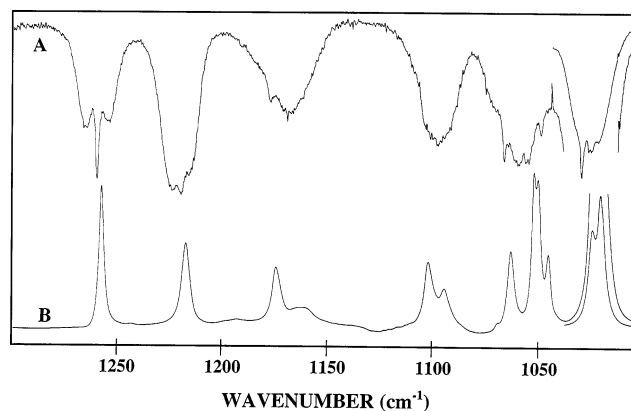


Figure 6. Infrared spectra in the region of 1000 to 1300 cm^{-1} of 1,1-dicyclopromethylene: (A) gas and (B) xenon solution at -70 °C.

the CH₂ antisymmetric and symmetric stretches; this is the order adopted in the earlier assignment, but the ab initio calculations predict this mode to be essentially accidentally degenerate with the CH₂ symmetric stretch. In terms of the bending modes, with a scaling factor of 0.9 the carbon–hydrogen deformations are predicted too high, but there is little question concerning these assignments based on the infrared spectra of the xenon solution. The predicted frequencies for two of the other =CH₂ bends (=CH₂ twist and =CH₂ rock) are observed 20 cm⁻¹ or more higher than the predicted values. The only place where there is some question concerning the order of a conformer pair is the two bands at 632 and 620 cm⁻¹, where the band in the infrared spectrum of the solid appears to originate from the 620 cm⁻¹ band in the xenon solution. However, since we have found that the predicted frequency order for modes of conformers of hydrocarbons is consistent with the observed order, we have assigned the lower frequency band of this pair to the C₂ conformer.

Once the fundamentals have been assigned for the C₁ form, there is little trouble in assigning the gauche-gauche (C₂) bands which disappear from the Raman spectrum of the liquid or from the infrared spectrum of the xenon solution when they are compared to the corresponding spectra of the solid. These assignments are listed in Table 2 along with the predicted values. Several weak bands could be assigned as fundamentals of the C₂ conformer but it is possible that several of these could be combination and/or overtone bands. Also many of the fundamentals for the C₂ form are nearly accidentally degenerate with similar modes of the more stable C₁ form.

A diligent search for evidence of the third conformer results in only two possibilities. The C=C in-plane bend fundamental is reasonably well separated for the three conformers. The one for the C₁ conformer is predicted at 403 cm⁻¹ and observed at 426 cm⁻¹. The corresponding C₂ band is predicted at 454 cm⁻¹ and observed at 476 cm⁻¹. There is a Q-branch at 415 cm⁻¹ that could be due to the gauche-gauche' (C_s) form (predicted at 400 cm⁻¹). Another possibility of identifying the C_s conformer lies with the strongest infrared band in the entire spectrum, the =CH₂ rock. The band at 883 cm⁻¹ could be due to the C_s rotamer but it is obscured by the much more intense fundamental of the most stable conformer at 879 cm⁻¹. Thus only very limited experimental evidence could be suggested for the presence of the third conformer.

Discussion

The MP2/6-31G(d) ab initio calculations with the two scaling factors predict the observed fundamentals for the C₁ conformer to within an average error of 10 cm⁻¹, which represents only a 0.75% error. This relatively small basis set with only two scaling factors predicts both the frequencies and the relative intensities of the infrared spectrum remarkably well and there is no distinct need to use multiple scaling factors for the spectroscopic predictions.

There is extensive mixing of the modes for the C₁ conformer even for the heavy atom modes. For example, the in-plane ring breathing mode has 40% S₁₂ and 22% S₃₈ for the fundamental at 1198 cm⁻¹, whereas for the out-of-plane motion at 1192 cm⁻¹ the contributions are 37% S₃₈ and 21% S₁₂. The CH₂ twists, CH₂ rocks, and the heavy atom bends involve extensive mixing with significant contributions from four or more symmetry coordinates (Table 1). Therefore, the descriptions for several of these modes are rather arbitrary, but for many of the other ones the major contribution is greater than 50% and the approximate descriptions provide a reasonable view of the

nuclear motions. Of course the mixing is significantly reduced for the C₂ and C_s conformers because of the symmetry (Tables 2 and 3).

Since the structural parameters for the conformers differ very little, the corresponding force constants are nearly the same for all three conformers; in addition, the mixing for the low-frequency skeletal bends is also similar among the conformers. Therefore, there is little difference in the frequencies of the corresponding modes for the three conformers. The major differences in going from the trans-gauche (C₁) to gauche-gauche (C₂) form are for the force constants of the ∠C₁C₂C₃, ∠C₁C₄C₁₀, and ∠C₃C₁C₄ bends which decrease by 11%, 16%, and 23%, respectively. On the other hand, the ∠C₁C₃C₇ bend force constant increases by 21% whereas that for the ∠C₁C₃C₈ bend increases by 17%. These changes reflect the significant change in angles when the trans cyclopropyl ring rotates to the gauche position. There are some significant changes (11%) in the force constants for the ∠C₁C₄H₆ and ∠C₈C₃H₅ bends, but for most of the other force constants the changes are less than 2% for the corresponding ones between the C₁ and C₂ conformers.

Of major interest in this research is the conformational stability wherein the initial vibrational investigation it was concluded that only one conformer was present in the fluid phases and it was the cis-cis (C_{2v}) form that was consistent with the predicted stability from MINDO/3 calculations.³² However, from an initial electron diffraction investigation,³³ it was not possible to identify the conformation but an ab initio calculation with the 4-31G basis set³⁴ predicted the gauche-gauche (C₂) form as the most stable conformer. This conclusion was also reached in a more recent electron diffraction study¹⁹ where the conformer stability was determined to be 59% gauche (47% gauche-gauche, C₂, and 11% gauche-gauche', C_s) and 41% trans-gauche (C₁). Our results are in contrast to all of these earlier results where clearly the trans-gauche (C₁) form is the only one remaining in the annealed solid, and this form is more stable in liquid xenon where the determined Δ*H* value is expected to be near the value in the gas.^{35–39} The Δ*H* of 146 ± 30 cm⁻¹ is sufficiently large that the small association with xenon can have little differential effect on the two most abundant conformers since they have similar values of dipole moments. Therefore we believe the electron diffraction results are in error and probably resulted from heavy reliance on the low-to-medium level ab initio predicted stability where the calculations were performed with very small basis sets, apparently with frozen core treatment. We carried out similar calculations with the same basis set with (full) electron correlation and the C₂ conformer is predicted more stable by only 9 cm⁻¹ (Table 4) rather than the value of 73 cm⁻¹ that was reported¹⁹ earlier. On the low end of our calculations, the Hartree–Fock method predicted the C₂ form to be more stable by more than 250 cm⁻¹! Also for a molecule as large as 1,1-dicyclopropylethene, there are so many structural parameters that the theoretical diffraction curves for the C₁, C₂, and C_s forms become very similar, so obtaining the relative amounts of the three conformers by means of numerous band deconvolutions must be a daunting task, which is why the earlier electron diffraction study¹⁹ did not give definitive curve fitting results.

To support the Δ*H* value obtained from the variable-temperature infrared spectra, we also calculated the enthalpy difference between the C₁ and C₂ conformers utilizing a single temperature and the predicted infrared intensities from the MP2-(full)/6-31G(d) ab initio calculations. Then enthalpy difference is determined by the equation Δ*H* = -*kT* ln[(*g*_{C₁}·*I*_{C₂}·*ε*_{C₁})/(*g*_{C₂}·

$I_{C_1 \cdot \epsilon_{C_2}}]$, where g is the degeneracy of each conformer, I is the observed infrared intensity, and ϵ is the ab initio predicted infrared intensity. Given statistical weights $g_{C_1}/g_{C_2} = 2$, the equation is reduced to $\Delta H = -kT \ln[2(I_{C_2 \cdot \epsilon_{C_1}})/(I_{C_1 \cdot \epsilon_{C_2}})]$. By utilizing the peak heights from four conformer pairs at the lowest temperature where the bands are the sharpest, we obtained a value of 124 cm^{-1} , which is well within the experimental value of $146 \pm 30 \text{ cm}^{-1}$. We have used this method for some organophosphorus molecules where as many as 12 conformer pairs were utilized and the results were always within the totally experimentally determined values from the variable-temperature van't Hoff plot, so long as certain predicted intensities which have been known to involve large systematic errors from MP2 calculations were dropped. However, it should be noted that this method works only if the predicted intensities are reasonable and many conformer pairs are available.

The failure to recognize the presence of conformers in the earlier vibrational study¹⁶ was partially due to the fact that most of the fundamentals for the three conformers have nearly the same frequencies. Only five bands had significantly different frequencies from the most stable conformer and they were obviously missing in the spectrum of the solid. Presumably these earlier investigators did not consider the disappearance of these five bands sufficient to postulate the presence of a second conformer in the liquid. By using the ΔH of 146 cm^{-1} for the C_2 form and the predicted average of 350 cm^{-1} for the C_s form, estimated conformation abundance was obtained at ambient temperature with 75% C_1 , 19% C_2 , and 6% C_s . As suggested earlier,¹⁹ it is interesting to compare the relative conformer stability of the 1,1-dicyclopentylene to that of the corresponding monosubstituted molecule, i.e., vinylcyclopropane, which exists mainly as the trans conformer (77% trans, 23% gauche).⁴⁰ If the disubstituted molecule is considered to be constructed from vinylcyclopropane with an additional cyclopropyl group, and if the trans-trans conformer of the disubstituted molecule is considered unacceptable, a mixture of 77% of the trans-gauche and 23% of the gauche-gauche form would be anticipated. This assumes that the two cyclopropyl groups have negligible interaction. These are nearly the values we obtained in this study, which indicates very little steric repulsion between the trans and gauche cyclopropyl groups.

The stable conformers of 1,1-dicyclopentylene are in contrast to those of dicyclopentyl ketone where the most stable conformer is the cis-cis (C_{2v}) conformer (C=O bond over the two three-membered ring). The minor conformer ($13 \pm 2\%$ at ambient temperature) is the cis-trans (C_s) form where the C=O bond is eclipsing the hydrogen atom on one of the rings. The enthalpy difference between these two conformers has been determined to be $530 \pm 27 \text{ cm}^{-1}$ ($6.34 \pm 0.32 \text{ kJ} \cdot \text{mol}^{-1}$) and the theoretical predictions are consistent with these experimental results. These significantly different conformational stabilities between these two isoelectronic molecules clearly show the steric effect of the hydrogen atoms on the ethene part of 1,1-dicyclopentylene where a cis form is not even present.

The asymmetric cyclopropyl torsional potential has been predicted from ab initio calculations. Beginning at the minimum for the most stable trans-gauche conformer, a potential function was determined by keeping one cyclopropyl group in the gauche position with respect to the double bond (dihedral $\sim 60^\circ$) while rotating the other cyclopropyl group (starting from trans position, dihedral $\sim 180^\circ$) at 30° intervals throughout a 360° cycle. The energies were calculated with full optimization of all structural parameters, except for the varying dihedral angle at increments of 30° , at each point from MP2(full)/6-31G(d) and MP2(full)/

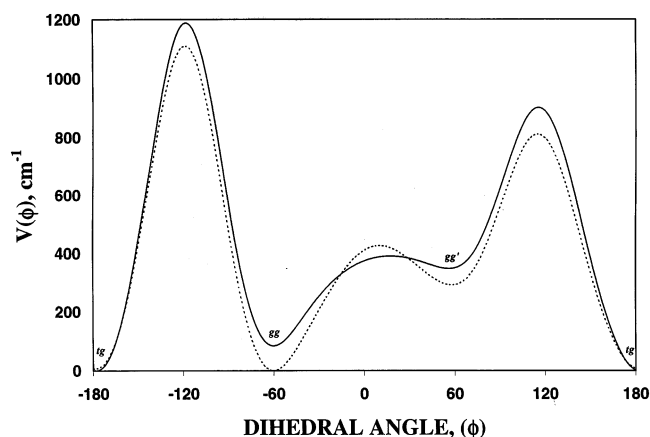


Figure 7. Asymmetric torsional potential function for 1,1-dicyclopentylene. The solid curve corresponds to the potential function calculated at the MP2(full)/6-311G(d,p) level and the dotted curve corresponds to the one calculated at the MP2(full)/6-31G(d) level. A torsional dihedral angle of ca. 180° corresponds to the most stable trans-gauche conformer, ca. -60° the second most stable gauche-gauche conformer, and ca. 60° the least stable gauche-gauche' conformer.

TABLE 7: Calculated Potential Barriers and Fourier Potential Coefficients of 1,1-Dicyclopentylene

	MP2(Full)/ 6-31G(d)	MP2(Full)/ 6-311G(d,p)
coeff (cm^{-1})		
V_1	186	207
V_2	349	447
V_3	-672	-671
V_4	106	140
V_5	84	92
V_6	-38	-36
V'_1	34	21
V'_2	251	217
V'_3	2	6
V'_4	-98	-107
V'_5	44	37
potential barriers (cm^{-1})		
$tg \rightarrow gg$	1103	1188
$tg \rightarrow gg'$	805	902
$gg \rightarrow tg$	1110	1104
$gg \rightarrow gg'$	427	307
$gg' \rightarrow tg$	519	554
$gg' \rightarrow gg$	135	43

6-311G(d,p) calculations. All three stable conformers appear as minima on the plot, i.e., dihedral angles $\sim 180^\circ$, $\sim -60^\circ$, and $\sim 60^\circ$ correspond to the trans-gauche, gauche-gauche, and gauche-gauche' conformers, respectively. Two of the three maxima correspond to alternative C_2 and C_s symmetry forms where the gauche dihedral angles are $\sim 120^\circ$ rather than $\sim 60^\circ$ in the stable conformers, the cis-gauche orientation (dihedral $\sim 0^\circ$) is also predicted to be a maximum, although it is the lowest energy transition state. The calculated potential functions are shown in Figure 7. Utilizing a Fourier cosine and sine series to represent the asymmetric potential function with the form $V(\phi) = \sum_{i=1}^6 (V_i/2)(1 - \cos i\phi) + \sum_{i=1}^5 (V'_i/2)(\sin i\phi)$, the potential constants for the first six cosine terms and the first five sine terms were obtained. The potential constants, calculated at MP2(full)/6-31G(d) and MP2(full)/6-311G(d,p) levels, are listed in Table 7. Of particular interest is the extremely small predicted value for the gauche-gauche' to gauche-gauche barrier of only 43 cm^{-1} from the MP2(full)/6-311G(d,p) calculation, which is the lowest MP2 level to yield correct conformational stability. For the gauche-gauche' form, the A' torsional fundamental, which is predicted to be 10 times more intense than the corresponding A'' mode, is predicted at 68 cm^{-1} . This value

plus the zero-point energy is more than two times larger than the MP2(full)/6-311G(d,p) predicted potential barrier, which suggests the gauche-gauche' well may be too shallow to withhold the vibrational transition between the ground and the virtual first excited state. This, along with the large energy difference between the gauche-gauche' form and the most stable trans-gauche conformer, may account for the lack of spectroscopic evidence for the presence of the gauche-gauche' form.

The predicted structural parameters for the trans and gauche cyclopropyl groups are remarkably similar. For example, the C₁–C₃ (gauche) and C₁–C₄ (trans) distances only differ by 0.004 Å between the two groups (Table 5). Similarly the opposite C₇–C₈ (gauche) and C₉–C₁₀ (trans) distances in the rings differ by only 0.003 Å with the one in the gauche position having the longer distance, the same as what was found for the attached carbon–carbon bond in similar molecules. The ∠C₄C₁C₂ is predicted to be 3° smaller for the trans cyclopropyl group compared to the corresponding angle for the gauche one whereas the ∠C₃C₁C₄ opens about 4° for the C₁ conformer compared to the similar angles for the other two conformers.

We have found for several monosubstituted cyclopropyl molecules^{15,20,41} the ab initio MP2(full)/6-311+G(d,p) predicted heavy atom parameters need to be adjusted by only 0.002 to 0.003 Å, and the adjusted of carbon–hydrogen distances are no more than 0.002 Å of the reported values, to fit the reported microwave rotational constants. Therefore it is believed that the adjusted *r*₀ structural parameters listed in Table 5 are more accurate than those obtained from the electron diffraction study. If one takes the average of the three different carbon–carbon distances for the trans cyclopropyl group, one obtains the average 1.512 Å, which is the same value as reported from the recent electron diffraction study¹⁹ and is only 0.001 Å longer than the average in the gauche cyclopropyl group. However, we would like to point out that the predicted differences of as much as 0.012 Å for some of these bonds within a ring is undoubtedly a realistic difference.

Acknowledgment. J.R.D. acknowledges the University of Missouri–Kansas City for a Faculty Research Grant for partial financial support of this research. C.J.W. is grateful for the support provided by a development leave that allowed him to assist in carrying out this research.

Supporting Information Available: Table 1S, scaled diagonal force constants from MP2(full)/6-31G(d) ab initio calculations for 1,1-dicyclopropylethene; and Table 2S, symmetry coordinates of 1,1-dicyclopropylethene. This material is available free of charge via the Internet at <http://pubs.acs.org>.

References and Notes

- (1) Volltrauer, H. N.; Schwendeman, R. H. *J. Chem. Phys.* **1971**, *54*, 260.
- (2) Bartell, L. S.; Guillory, J. P. *J. Chem. Phys.* **1965**, *43*, 647.
- (3) Durig, J. R.; Bist, H. D.; Little, T. S. *J. Chem. Phys.* **1988**, *61*, 529.
- (4) Durig, J. R.; Feng, F.; Little, T. S.; Wang, A. *Struct. Chem.* **1992**, *3*, 417.
- (5) Durig, J. R.; Shen, S. *Spectrochim. Acta A* **2000**, *56*, 2545.
- (6) Lüttke, W.; De Meijere, A. *Angew. Chem., Int. Ed. Engl.* **1966**, *5*, 512.
- (7) Günther, H.; Wendisch, D. *Angew. Chem., Int. Ed. Engl.* **1966**, *5*, 251.
- (8) De Mare, G. R.; Martin, J. S. *J. Am. Chem. Soc.* **1966**, *88*, 5033.
- (9) Günther, H.; Klose, H.; Cremer, D. *Chem. Ber.* **1971**, *104*, 3884.
- (10) De Meijere, A.; Lüttke, W. *Tetrahedron* **1969**, *25*, 2047.
- (11) Hehre, W. J. *J. Am. Chem. Soc.* **1972**, *94*, 6592.
- (12) Codding, E. G.; Schwendeman, R. H. *J. Mol. Spectrosc.* **1974**, *49*, 226.
- (13) Carreira, L. A.; Towns, T. G.; Malloy, T. B., Jr. *J. Am. Chem. Soc.* **1978**, *100*, 385.
- (14) Salares, V. R.; Murphy, W. F.; Bernstein, H. J. *J. Raman Spectrosc.* **1978**, *7*, 147.
- (15) Wurrey, C. J.; Zheng, C.; Guirgis, G. A.; Durig, J. R. *Phys. Chem. Chem. Phys.* **2004**, *6*, 2125.
- (16) Nease, A. B.; Wurrey, C. J. *J. Phys. Chem.* **1979**, *83*, 2135.
- (17) Andrieu, C. G.; Paquer, D.; Mollier, Y. *C. R. Acad. Sci. Paris Ser. C* **1973**, *276*, 927.
- (18) Aroney, M. J.; Calderbank, K. E.; Stootman, H. J. *J. Chem. Soc., Perkin Trans.* **1973**, *2*, 1365.
- (19) Traetteberg, M.; Bakken, P.; Quesada, J. V.; Mastryukov, V. S.; Boggs, J. E. *J. Mol. Struct.* **1999**, *485/486*, 73.
- (20) Durig, J. R.; Yu, Z.; Zheng, C.; Guirgis, G. A. *J. Phys. Chem. A* **2004**, *108*, 5353.
- (21) Durig, J. R.; Shen, S.; Zhu, X.; Wurrey, C. J. *J. Mol. Struct.* **1999**, *485*, 501.
- (22) Wurrey, C. J.; Shen, S.; Gounev, T. K.; Durig, J. R. *J. Mol. Struct.* **1997**, *405*, 207.
- (23) Wurrey, C. J.; Shen, S.; Zhu, X.; Zhen, H.; Durig, J. R. *J. Mol. Struct.* **1998**, *449*, 203.
- (24) Guirgis, G. A.; Wurrey, C. J.; Yu, Z.; Zhu, X.; Durig, J. R. *J. Phys. Chem. A* **1999**, *103*, 1509.
- (25) Frisch, M. J.; Trucks, G. W.; Schlegel, H. B.; Scuseria, G. E.; Robb, M. A.; Cheeseman, J. R.; Montgomery, J. A., Jr.; Vreven, T.; Kudin, K. N.; Burant, J. C.; Millam, J. M.; Iyengar, S. S.; Tomasi, J.; Barone, V.; Mennucci, B.; Cossi, M.; Scalmani, G.; Rega, N.; Petersson, G. A.; Nakatsuji, H.; Hada, M.; Ehara, M.; Toyota, K.; Fukuda, R.; Hasegawa, J.; Ishida, M.; Nakajima, T.; Honda, Y.; Kitao, O.; Nakai, H.; Klene, M.; Li, X.; Knox, J. E.; Hratchian, H. P.; Cross, J. B.; Adamo, C.; Jaramillo, J.; Gomperts, R.; Stratmann, R. E.; Yazyev, O.; Austin, A. J.; Cammi, R.; Pomelli, C.; Ochterski, J. W.; Ayala, P. Y.; Morokuma, K.; Voth, G. A.; Salvador, P.; Dannenberg, J. J.; Zakrzewski, V. G.; Dapprich, S.; Daniels, A. D.; Strain, M. C.; Farkas, O.; Malick, D. K.; Rabuck, A. D.; Raghavachari, K.; Foresman, J. B.; Ortiz, J. V.; Cui, Q.; Baboul, A. G.; Clifford, S.; Cioslowski, J.; Stefanov, B. B.; Liu, G.; Liashenko, A.; Piskorz, P.; Komaromi, I.; Martin, R. L.; Fox, D. J.; Keith, T.; Al-Laham, M. A.; Peng, C. Y.; Nanayakkara, A.; Challacombe, M.; Gill, P. M. W.; Johnson, B.; Chen, W.; Wong, M. W.; Gonzalez, C.; Pople, J. A. *Gaussian 03*, revision B.04; Gaussian, Inc.: Pittsburgh, PA, 2003.
- (26) Pulay, P. *Mol. Phys.* **1969**, *17*, 197.
- (27) Guirgis, G. A.; Zhu, X.; Yu, Z.; Durig, J. R. *J. Phys. Chem. A* **2000**, *104*, 4383.
- (28) Frisch, M. J.; Yamaguchi, Y.; Gaw, J. F.; Schaefer, H. F., III; Binkley, J. S. *J. Chem. Phys.* **1986**, *84*, 531.
- (29) Amos, R. D. *Chem. Phys. Lett.* **1986**, *124*, 376.
- (30) Polavarapu, P. L. *J. Phys. Chem.* **1990**, *94*, 8106.
- (31) Chantry, G. W. In *The Raman Effect*; Anderson, A., Ed.; Marcel Dekker Inc.: New York, 1971; Vol. 1, Chapter 2.
- (32) Dewar, M. J. S.; Fonken, G. J.; Jones, T. B.; Minter, D. E. *J. Chem. Soc., Perkin Trans.* **1976**, *2*, 764.
- (33) Sugawara, Y.; Konaka, S.; Tamagawa, T.; Kimura, M. *Symposium on Molecular Structures*, October 1979, Tokyo, Japan.
- (34) Takeshita, K. *J. Mol. Struct.* **1985**, *133*, 161.
- (35) Bulanin, M. O. *J. Mol. Struct.* **1973**, *19*, 59.
- (36) Van der Veken, B. J.; DeMunck, F. R. *J. Chem. Phys.* **1992**, *97*, 3060.
- (37) Herrebout, W. A.; Van der Veken, B. J.; Wang, A.; Durig, J. R. *J. Phys. Chem.* **1995**, *99*, 578.
- (38) Bulanin, M. O. *J. Mol. Struct.* **1995**, *347*, 73.
- (39) Herrebout, W. A.; Van der Veken, B. J. *J. Phys. Chem.* **1996**, *100*, 9671.
- (40) Traetteberg, M.; Bakken, P.; Almenningen, A.; Lüttke, W. *J. Mol. Struct.* **1988**, *189*, 357.
- (41) Durig, J. R.; Zheng, C.; Warren, R. D.; Groner, P.; Wurrey, C. J.; Gounev, T. K. *J. Phys. Chem. A* **2003**, *107*, 7713.